Numerical Investigation of Quenching for a Nonlinear Diffusion Equation with a Singular Neumann Boundary Condition

C. I. Christov, K. Deng
Department of Mathematics, University of Louisiana at Lafayette, Lafayette, Louisiana 70504-1010

Received 26 July 2001; revised 3 October 2001; accepted 3 October 2001

For a nonlinear diffusion equation with a singular Neumann boundary condition, we devise a difference scheme which represents faithfully the properties of the original continuous boundary value problem. We use non-uniform mesh in order to adequately represent the spatial behavior of the quenching solution near the boundary. © 2002 Wiley Periodicals, Inc. Numer Methods Partial Differential Eq 18: 429–440, 2002; Published online in Wiley InterScience (www.interscience.wiley.com); DOI 10.1002/num.10013

Keywords: nonlinear diffusion equation; Neumann boundary condition; energy balanced difference schemes

1. INTRODUCTION

Nonlinear problems in thermal conductivity are of prime interest in many areas of physics. Nonlinearities can arise in the heat-conduction equation itself and/or in the boundary conditions. The former occurs when there exist internal sources of heat in the region under consideration. The latter encompasses the situations when there is radiation from the surface into an effective continuous medium. Then the boundary condition for the temperature u reads (see, e.g., [1]):

$$\kappa \frac{\partial u}{\partial n} = \sigma(u^4 - u_0^4),$$

which leads to blow-up on the boundary since the power of u is greater than unity. A reversed situation is encountered in thermoconvective boundary layers when the temperature gradient can become at certain moment of time unfavorable for the local convective motion. Since the eddy coefficient of heat diffusion κ and resistance coefficient σ are functionals of the temperature distribution then locally the following condition:

Correspondence to: C. I. Christov, Department of Mathematics, University of Louisiana at Lafayette, P.O. Box 1010, Lafayette, LA 70504-1010 (e-mail: christov@louisiana.edu)
Contract grant sponsor: La SPACE Consortium; contract grant number: R199524
under LEGSF and NASA, contract grant number: NGT5-40035.

$$\frac{\partial u}{\partial n} = Cu^{\alpha} - F(u_0), \tag{1.1}$$

can provide the most pertinent physical model for the effective thermal interaction of the convected medium and the boundaries. Note that the coefficient of laminar heat diffusion is neglected, which is a reasonable approximation during the periods with dominant eddy diffusivity. For $\alpha < 0$ a process of quenching of the temperature can be incited. Naturally the coefficient of eddy diffusion will decrease with the decrease of the temperature and ultimately one is to consider the coefficient of laminar diffusion. Yet, there is a significantly long period of time during which Eq. (1.1) gives the first-order effect. A typical physical situation is the formation of inverse layers within the atmospheric boundary layer, which can hinder the natural ability of the atmosphere to diffuse smog particles. For a discussion on this topic, see [2].

Recently, modeling the unsteady thermoconvective flows in vertical slots has attracted attention because of applications to flows under reduced gravity with significant influence of the modulation part of the gravity acceleration. This is the so-called *G*-jitter flow (see, e.g., [3] and the literature cited therein). Because of the unsteady loading forces, there take place periods of time during which the temperature gradient at the wall is unfavorable and a process of quenching can take place. The blow-up scenario is also of interest, but it requires different numerical technique and will be treated elsewhere.

The objective of the present work is twofold. First, we investigate the theoretical conditions under which quenching takes place. Second, we gather some insight about the behavior of the solution for the temperature before embarking on a full-fledged numerical simulation of *G*-jitter with nonlinear Neumann boundary condition. This is the applied aspect of the motivation of the present work.

2. POSING THE PROBLEM

The problem under consideration is as follows:

$$\gamma u^{\gamma-1} u_t = u_{xx} \qquad 0 < x < 1, \quad 0 < t < T, \tag{2.1}$$

$$u_x(1,t) = 0,\ u_x(0,t) = u^{-\beta}(0,t) \qquad 0 < t < T, \tag{2.2}$$

$$u(x,0) = u_0(x) \qquad 0 \le x \le 1, \tag{2.3}$$

where $\gamma > 0$ and $\beta > 0$ are real numbers. As is well known, if $0 < \gamma < 1$, (2.1) is the porous medium equation; if $\gamma > 1$, (2.1) is a plasma type equation; if $\gamma = 1$, it reduces to the ubiquitous heat equation. Such a problem was originally studied in [4] for the limiting case of linear heat-conduction equation $\gamma = 1$. In [5] the quenching behavior of the solution was examined, that is, the solution reaches zero in a finite time (note that the solution must be positive). To motivate our discussion in the present article, we recall two main results from [5]:

Theorem A (Finite Quenching). *Every solution of* (2.1)–(2.3) *quenches in a finite time under the following assumptions on the initial data*:

$$u_0(x) \ge 0, \quad u_0'(x) \ge 0, \quad u_0''(x) \le 0, \tag{2.4}$$

and the "*compatibility conditions*"

$$u_0'(1) = 0, \quad u_0'(0) = u_0^{-\beta}(0). \tag{2.5}$$

Moreover, the quenching occurs only on the boundary, i.e., at $x = 0$.

Theorem B (Quenching Rate). *Suppose that*

$$u_0'(x) \geq 0 \quad \text{and} \quad u_0''(x) \leq 0.$$

Then the solution of (2.1)–(2.3) *satisfies*

$$C_1 \leq u(0,t)(T-t)^{[1/(\gamma+2\beta+1)]} \leq C_2, \tag{2.6}$$

where C_1 *and* C_2 *are positive numbers, and* T *is the quenching time.*

It is worth mentioning that for $\gamma = 1$, these results had been established in [6]. However, from technical point of view, the results of [6] are somewhat different from those in [5]. On the one hand, in Theorem A of [6], no assumptions are imposed on the initial data, except the compatibility conditions. On the other hand, in Theorem B of [6], more restrictive conditions are assumed.

From the above observations, a natural question arises: Without assumptions on u_0, can Theorems A and B of [5] still hold? To our knowledge, no analytical arguments have been used to answer the question at this stage. Therefore, in the present article we devise a difference scheme. The guiding principle when constructing the scheme was that it faithfully represents the balance for the energy the same way as the original continuous equation does.

To verify the result of Theorem A, we consider four different initial conditions. Some of them satisfy the conditions of the theorem, whereas the other do not.

(i) An initial condition that satisfies behavioral conditions (2.4) and the compatibility conditions (2.5) reads

$$u_0(x) = a\cos(1-x), \quad a = [\sin(1)\cos^{\beta}(1)]^{-[1/(\beta+1)]}, \quad x \in [0,1]. \tag{2.7}$$

(ii) An initial condition that satisfies the compatibility conditions and first two of the behavioral conditions is the following:

$$u_0(x) = -4x^3 + 3x^2 + 6x + 6^{-(1/\beta)}, \quad x \in [0,1]. \tag{2.8}$$

(iii) An initial condition that satisfies the compatibility conditions and only the first of the behavioral conditions is given by

$$u_0(x) = \cos(6) - \cos(6(1-x)) + (-6\sin(6))^{-(1/\beta)}, \quad x \in [0,1]. \tag{2.9}$$

(iv) An initial condition satisfying the behavioral condition (2.4) but not satisfying the nonlinear compatibility condition is simply a constant. For definiteness we choose

$$u_0(x) = 1.483, \quad x \in [0,1] \tag{2.10}$$

3. DIFFERENCE SCHEME

3.1. Nonuniform Grid and Spatial Discretization

When quenching occurs near the point $x = 0$ the gradients of the solution become very large. It is easy to show that the behavior of the solution near the point $x = 0$ at the moment of quenching obeys the rule

$$u \sim [(1 + \beta)x]^{1/(1+\beta)} \tag{3.1}$$

because in that moment one has $u = 0$. This kind of local behavior of the solution requires a nonuniform grid because of the steep increase of the sought function u. In fact, most of the time a uniform grid would be sufficient because $u(0, t) \neq 0$. Yet, in order to capture the quenching moment with high accuracy, one needs a grid that is adequately dense even for the last moment of calculations, namely for $t = T_c$, where T_c is the quenching time.

There is no real need for a time-dependent grid whose spacings change dynamically during the evolution. It could eventually save a couple of grid points on the initial stages when u is nonsingular at $x = 0$, but recalculating the functional values at each time step will require costly interpolation procedures and will inevitably introduce additional truncation error, which will prevent us from devising a scheme with exact difference satisfaction of the energy balance.

To this end we introduce the following coordinate transformation:

$$\xi = [(1 + \beta)x]^{1/(1+\beta)}, \quad \frac{d\xi}{dx} \sim [(1 + \beta)x]^{-\beta/(1+\beta)} \rightarrow \frac{dx}{d\xi} \sim [(1 + \beta)x]^{\beta/(1+\beta)},$$

which secures that

$$\frac{du}{d\xi} = \frac{du}{dx}\frac{dx}{d\xi} \sim [(1 + \beta)x]^{-\beta/(1+\beta)}[(1 + \beta)x]^{\beta/(1+\beta)} \sim O(1). \tag{3.2}$$

Thus the pointwise change of the solution u as a function of the independent variable ξ will be approximately uniform near the quenching point $x = 0$. The latter means that the approximation will be uniform.

The above consideration allows us to set for our problem a nonuniform grid which does not depend on time. In the cases when the quenching point is not known in advance the nonuniform grid (the coordinate transformation) has to be defined *a posteriori,* i.e., it has to change during the time-stepping of the solution.

In terms of the independent variable ξ we use a staggered uniform grid:

$$\xi_i = h_0(i - 1.5), \quad i = 1,2, \ldots ,M, \quad h_0 = \frac{1}{M - 2}.$$

In the original domain (coordinate x) the grid points are prescribed by the following difference function:

$$x_i = [h_0(i - 1.5)]^{(1+\beta)}, \quad i = 2, \ldots ,M - 1, \quad x_1 = -x_2, x_M = 2 - x_{M-1}, \tag{3.3}$$

which means that the boundary $x = 0$ is situated exactly in the middle between the first and second grid points, whereas the boundary $x = 1$ is in the middle between the last two points. This is important for the second-order approximation of boundary conditions that involve derivatives. For the nonuniform x-spacing h_i we get the following expression:

$$h_{i+1} = x_{i+1} - x_i, \quad i = 1, \ldots, M-1.$$

It is clear that the grid (3.3) is denser near the boundary $x = 0$ where the solution is expected to be proportional to $x^{1/(1+\beta)} (1/(1+\beta) < 1)$ in the late stages of quenching. This way we have adequate number of grid points to capture the behavior. Then the error of the spatial discretization is practically uniform (see also (3.2)).

On the nonuniform grid the difference approximation for the second spatial derivative reads

$$\Lambda u_i \underline{\underline{\text{def}}}\ 2\left[\frac{h_i u_{i+1} - (h_i + h_{i+1})u_i + h_{i+1}u_{i-1}}{h_i h_{i+1}(h_i + h_{i+1})}\right] = u''(x_i) + O(h_{i+1} - h_i). \tag{3.4}$$

In the case under consideration the spacings h_i can be considered as the grid values of certain continuous function $h(\xi_i)$. Hence a simple expression of h_{i+1} in Taylor series at the point ξ_i shows that the difference scheme on the nonuniform grid is of second order of approximation.

3.2. Temporal Discretization

Denote by τ the time increment. The superscript n on the time variable t stands for the current ("old") time stage, and $n + 1$ for the "new" one. The following scheme akin to Crank-Nicholson scheme is used:

$$\frac{2}{\gamma + 1}\left[\frac{(u_i^{n+1})^{\gamma+1} - (u_i^n)^{\gamma+1}}{(u_i^{n+1})^2 - (u_i^n)^2}\right]\frac{u_i^{n+1} - u_i^n}{\tau} = \frac{1}{2}\Lambda[u_i^{n+1} + u_i^n], \tag{3.5}$$

where Λ is the difference operator defined in (3.4).

The scheme (3.5) is nonlinear and cannot be implemented without linearization. The simplest way to do this is to introduce iterations as follows:

$$\frac{2}{\gamma + 1}\left[\frac{(u_i^{n+1,k})^{\gamma+1} - (u_i^n)^{\gamma+1}}{(u_i^{n+1,k})^2 - (u_i^n)^2}\right]\frac{u_i^{n+1,k+1} - u_i^n}{\tau} = \frac{1}{2}\Lambda[u_i^{n+1,k+1} + u_i^n], \tag{3.6}$$

and to repeat them until convergence is reached in the sense that

$$\frac{\max_i \|u_i^{n+1,k+1} - u_i^{n+1,k}\|}{\max_i \|u_i^{n+1,k+1}\|} \le \varepsilon \approx 10^{-12}.$$

The decision to use iterations enables us to use a simplest linearization of the boundary condition at $x = 0$ which reads

$$u_2^{n+1,k+1} - u_1^{n+1,k+1} = h_2\left(\frac{u_2^{n+1,k} + u_1^{n+1,k}}{2}\right)^{-\beta}.$$

Thus at each iteration for the unknown function $u_i^{n+1,k+1}$ we are solving a boundary value problem that contains only its derivatives at the boundary points. Yet, the overall problem is correct because of the term stemming from the time derivative.

3.3. Organization of the Algorithm

As initial condition for the internal iterations we use the value of the function on the previous ("old") time step n. After the iterations converge we get the function on the "new" time stage $n + 1$. Then we move to the next time step, etc.

Special care is taken to refine the time increment τ when the solution approaches the moment of quenching. A step is executed with the current value of τ. If a negative value for $u(0, t)$ is encountered, then the time increment is reduced in half and the step is repeated until a positive value is the outcome of the calculations. If a positive value is not found for $\tau < 10^{-15}$, then the process is terminated.

The refining of the time increment can be also used in order to secure good approximation near the moment of quenching when the time derivative is rather large. We choose to decrease (increase) τ in a manner that the relative increase of $u(0, t)$ is a prescribed quantity. For different values of the governing parameters this quantity can vary, say from 10^{-6} to 10^{-2}.

4. DIFFERENCE REPRESENTATION OF THE ENERGY BALANCE

In this section we consider the nonlinear implicit difference scheme, which ensues from the above algorithm after the internal iterations converge. We show that it represents faithfully the energy balance as the continuous problem does. For linear problems this approach is elucidated in the monograph [7].

The scalar product is introduced as follows:

$$(\phi,\psi) = \sum_{i=2}^{M-1} \frac{h_i + h_{i+1}}{2}\, \phi_i \psi_i.$$

Then

$$(u,\Lambda u) = \sum_{i=2}^{M-1} u_i \left[\frac{h_i u_{i+1} - (h_i + h_{i+1})u_i + h_{i+1}u_{i-1}}{h_i h_{i+1}} \right]$$

$$= \sum_{i=2}^{M-1} \left[u_i \left(\frac{u_{i+1} - u_i}{h_{i+1}} \right) + u_i \left(\frac{-u_i + u_{i-1}}{h_i} \right) \right]$$

$$= -\frac{1}{2} \sum_{i=2}^{M-1} \left[\frac{u_i^2 + u_{i+1}^2 - 2u_i u_{i+1}}{h_{i+1}} \right] - \frac{1}{2} \sum_{i=2}^{M-1} \left[\frac{u_i^2 + u_{i-1}^2 - 2u_i u_{i-1}}{h_i} \right]$$

$$+ \frac{1}{2} \left(- \frac{u_{M-1}^2}{h_M} + \frac{u_M^2}{h_M} + \frac{u_1^2}{h_2} - \frac{u_2^2}{h_2} \right).$$

The boundary conditions (2.2) are approximated as follows (the quasi-linearization will be addressed later in the text):

$$u_M = u_{M-1}, \quad u_2 - u_1 = h_2\left(\frac{u_1 + u_2}{2}\right)^{-\beta}. \tag{4.1}$$

Then for the above scalar product we get

$$(u,\Lambda u) = -\frac{1}{2}\sum_{i=2}^{M-1}\left[h_{i+1}\left(\frac{u_i - u_{i+1}}{h_{i+1}}\right)^2 + h_i\left(\frac{u_i - u_{i-1}}{h_i}\right)^2\right] - \left(\frac{u_1 + u_2}{2}\right)^{1-\beta}. \tag{4.2}$$

The term containing the time derivative is nonlinear. This makes the scheme (3.5) faithfully represent the properties of the original initial-boundary value problem, e.g., energy integral. To prove that we multiply both sides of (3.5) by $\frac{1}{2}[u_i^{n+1} + u_i^n](h_i + h_{i+1})$ and take the sum from $i = 2$ to $i = M - 1$. Thus, we get

$$\frac{2}{\tau(\gamma+1)}\left[\sum_{i=2}^{M-1}(u_i^{n+1})^{\gamma+1}\frac{h_i + h_{i+1}}{2} - \sum_{i=2}^{M-1}(u_i^n)^{\gamma+1}\frac{h_i + h_{i+1}}{2}\right] = ([u^{n+1} + u^n],\ \Lambda[u^{n+1} + u^n]), \tag{4.3}$$

which is an equivalent of the respective property of the differential boundary value problem. In other words, the energy-like sum ("integral") evolves because of the (un)balance of the dissipation and energy production at the boundary with the nonlinear boundary condition. In this sense, our scheme does not contribute artificial (scheme) properties.

5. RESULTS AND DISCUSSION

The problem under consideration depends on two governing parameters β and γ. Qualitative differences in the behavior of the solution can be expected only when β and γ change from values smaller than unity to greater than (or equal to) unity. For instance, smaller values of β correspond to a solution with weaker singularity at $x = 0$ according to the asymptotic behavior of the local solution (3.1). Larger values of γ require smaller time increments τ.

We consider the following four sets of values for the governing parameters:

- $\beta = 0.5 < 1$ and $\gamma = 0.5 < 1$
- $\beta = 0.5 < 1$ and $\gamma = 2 > 1$
- $\beta = 2 > 1$ and $\gamma = 2 > 1$
- $\beta = 2 > 1$ and $\gamma = 0.5 < 1$

5.1. Initial Conditions and Quenching (Theorem A)

First we begin with the case (2.7) when the initial condition satisfies all the conditions of Theorem A. For all four sets of values for the governing parameters we encountered quenching in our numerical calculations. We verified the second order of approximation using four

different resolutions $N = 100$, $N = 400$, $N = 1600$, and $N = 6400$. The differences between the profiles were of order $O(N^{-2})$ when calculated on two grids with N and $2N$ grid points, respectively. We found that $N = 1600$ was fully adequate for all cases presented here. In what follows the results are obtained with $N = 1600$ unless it is specifically given another number in the text.

It is interesting to see how pertinent the local solution (3.1) is. The spatial profile of the solution in the moment of quenching is presented in the Figure 1 for the high resolution $N = 1600$ and compared to the analytical expression for the local solution.

The asymptotic behavior of the calculated solution approaches the behavior of the singular local solution as $x \to 0$, which lends additional credibility to the results obtained here. Note the highly zoomed x-axis, which exaggerates even the slightest differences between the compared profiles.

The second case ($\beta = 0.5$, $\gamma = 2$) is rather similar to the first with the only difference being that the temporal evolution is faster. This fact has to be accounted for in the initial selection of the time increment.

The third case ($\beta = 2$, $\gamma = 2$) is harder to treat numerically because of the higher-order of the singularity near $x = 0$ at the moment of quenching. Its temporal evolution is also faster than the one of first case. Once again we observed quenching for all different initial conditions that we used. The result is presented in Fig. 2 for the region near the origin of the coordinate system where the quenching takes place because of the nonlinear boundary condition. As mentioned above the number of grid intervals is $N = 1600$ and the x-axis is zoomed. Even with this small number of grid intervals we get accurate results because the nonuniform grid is dense in the vicinity of the origin and coarse in the regions where the changes of the sought functions are moderate.

Next we treat the case (2.8). We find no qualitative difference in the behavior in the sense that quenching does occur and that it happens at the boundary with the nonlinear boundary condition. The only quantitative difference is the quenching time, which depends on the initial condition. Hence, quenching does take place even when the third of the behavioral restrictions on the initial condition is not satisfied.

Proceeding further, we consider (2.9) when two of the behavioral conditions are not satisfied. The scenario is once again the same, except for some quantitative difference in the quenching time. For the sake of diversity we consider this case for $\beta = 0.5$ and $\gamma = 2$. In Figure 3 the

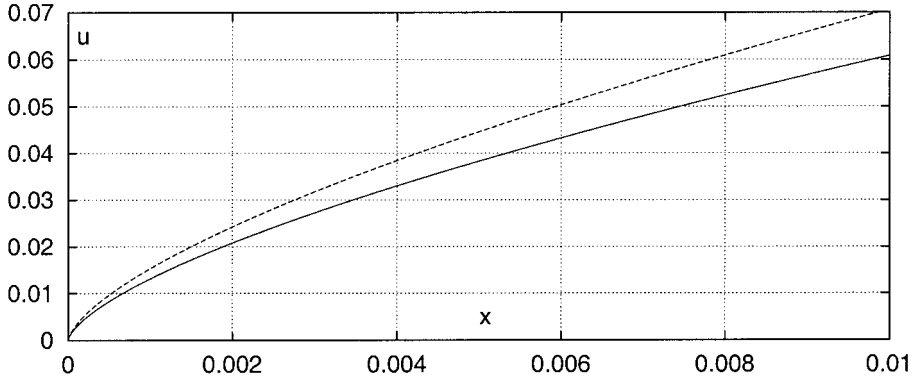

FIG. 1. The profile at the moment of quenching for $\beta = 0.5$, $\gamma = 0.5$, $N = 1600$. ----, computed; —, local analytical solution.

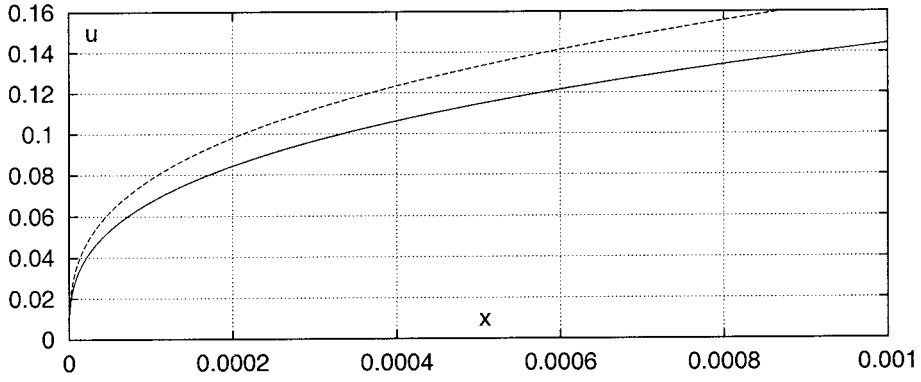

FIG. 2. The profile at the moment of quenching for $\beta = 2$, $\gamma = 2$, $N = 1600$. ----, computed; —, local analytical solution.

obtained solution $u(x, t)$ is presented as a surface plot. One can judge about the evolution of the time increment τ from the relative situation of the cross sections parallel to the plane of the initial condition.

We observed a similar behavior also for the constant initial condition (2.10).

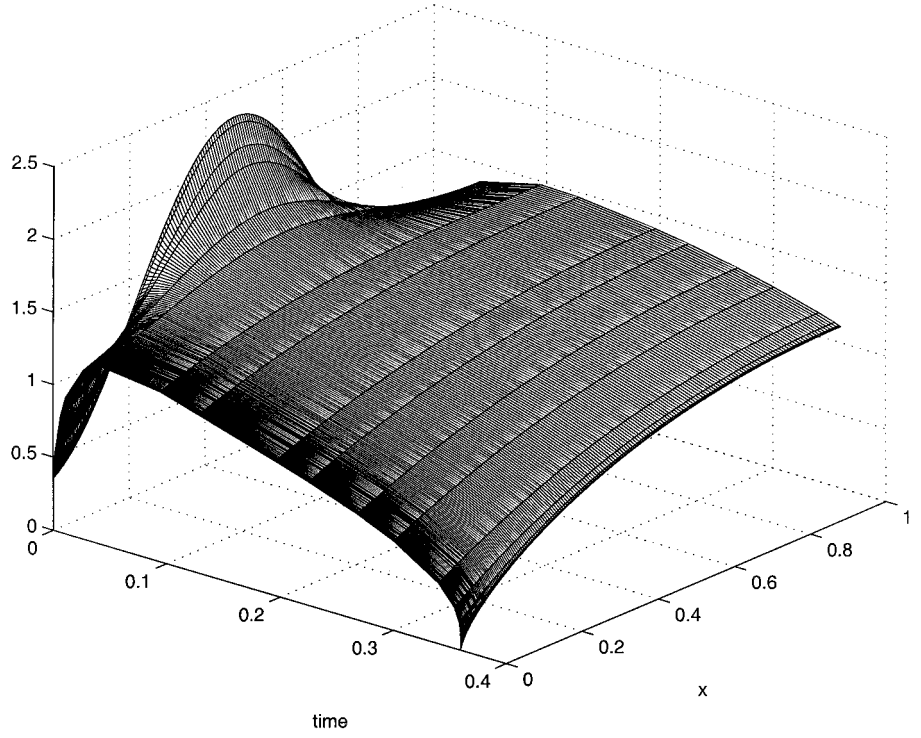

FIG. 3. Surface plot of function $u(x, t)$ for $\beta = 0.5$ and $\gamma = 2$.

5.2. Quenching Rate (Theorem B)

As quenching occurs for certain finite time $t = T$, the behavior of the function u is supposed to obey the law

$$u(0,t)(T-t)^{-[1/(\gamma+2\beta+1)]} \to C \quad \text{for} \quad t \to T, \tag{5.1}$$

or equivalently,

$$u(0,t) \sim C(T-t)^{[1/(\gamma+2\beta+1)]}, \quad u_t(0,t) \sim -\frac{C}{\gamma+2\beta+1}(T-t)^{[1/(\gamma+2\beta+1)]-1}. \tag{5.2}$$

Notice that since $\mu = 1/(\gamma + 2\beta + 1) < 1$, we have

$$u(0,t) \to 0, \quad u_t(0,t) \to -\infty \quad \text{for} \quad t \to T. \tag{5.3}$$

The finite difference version of (5.2) reads

$$u(0,t^n) = \tfrac{1}{2}(u_{1,n} + u_{2,n}) + O(\tau^2),$$

where the superscript n refers to the current time stage. In our compilations we collect data for $u(0, t)$ and then recast it into a different form (see Figs. 4 and 5).

In all of the cases under consideration quenching took place but the quenching time T depends on the actual shape of the initial condition. Hence a comparison explicitly involving T does not make much sense. For this reason after the process of quenching is completed and the quenching time established, we render $u(0, t)$ to $u(0, T - t)$ and present the results. In fact we extrapolate the quenching time T from the last two results for u, say u^N and u^{N-1}, where N is the number of time step immediately before the last time stage (the stage at which the quenching takes place). Then

$$T = \frac{(t^N - t^{N-1}R)}{(1-R)}, \quad R \overset{def}{=} \left(\frac{u^N}{u^{N-1}}\right)^{(\gamma+2\beta+1)}.$$

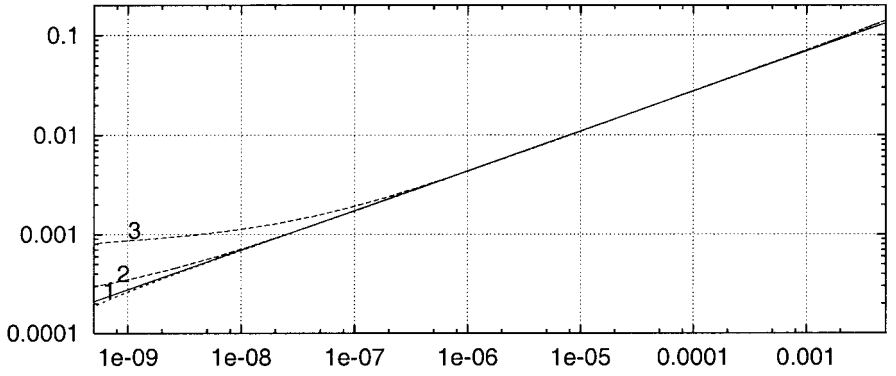

FIG. 4. Quenching rate for $\beta = 0.5$, $\gamma = 0.5$ (----). (1) $N = 6400$; (2) $N = 1600$; (3) $N = 400$. —, best-fit approximation $1.1(T - t)^{0.4}$.

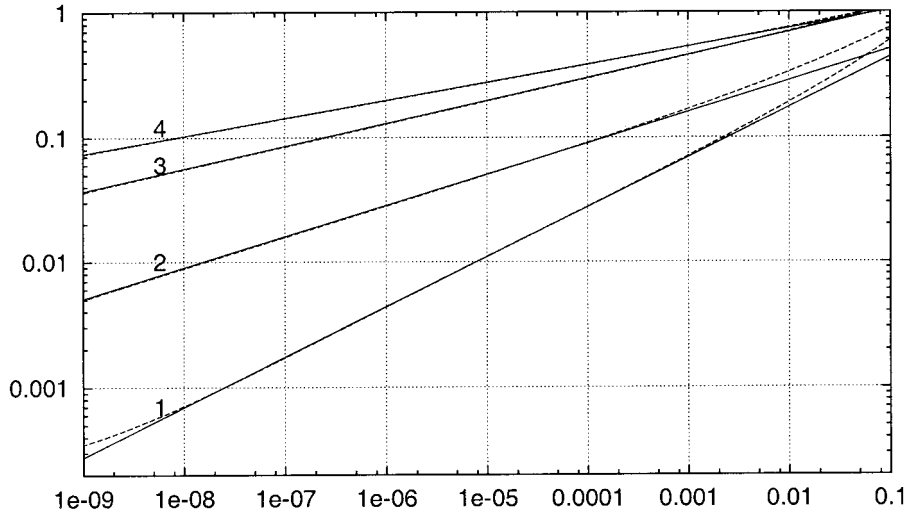

FIG. 5. Quenching rate for different sets of governing parameters. ----, the numerical calculations; — the respective best-fit approximations. (1) $\beta = 0.5$, $\gamma = 0.5$ ($u(0, t) = 1.1(T - t)^{1/2.5}$); (2) $\beta = 0.5$, $\gamma = 2$ ($u(0, t) = 0.9(T - t)^{1/4}$); (3) $\beta = 2$, $\gamma = 0.5$ ($u(0, t) = 1.6(T - t)^{1/5.5}$); (4) $\beta = 2$, $\gamma = 2$ ($u(0, t) = 1.43(T - t)^{1/7}$).

In the case $\gamma = 0.5$ and $\beta = 0.5$ we present in Fig. 4 the calculated $u(0, T - t)$ with three different resolutions. The best-fitting curve of type of (5.2) is juxtaposed to the numerical results. In this case the power in (5.2) is $(\gamma + 2\beta + 1)^{-1} = 0.4$.

As can be seen from the Fig. 4, the agreement for $u(0, t)$ between the calculations with different resolution is very good, and the finest mesh gives a result that fits the result of Theorem B quantitatively very well. The deviations for the rougher mesh are inevitable because of the fact that the solution near the boundary becomes so small that it is submerged into the truncation error.

Qualitatively the same is the situation with all of the four cases considered here. Figure 5 shows the results for the four cases with different dashed lines. The respective best-fit approximation is depicted with a solid line. It is clearly seen that in all of the cases the calculations confirm the expression for the behavior of u as derived in Theorem B.

6. CONCLUSIONS

For $\gamma \neq 1$ we have found numerically that all of the initial profiles inevitably lead to quenching, including the nonmonotone initial profiles, which do not satisfy the requirements of Theorem A. This kind of behavior of the solution is due to the presence of diffusion. The latter smooths the solution on the initial stage of the evolution, eventually transforming the spatial profile into a unimodal function of the spatial variable. Thus, the profile becomes reasonably close to the profiles that satisfy the conditions of Theorem A. Then a quick process of quenching begins.

This is similar to the analytical result of [6] for the linear diffusion equation $\gamma = 1$ under nonlinear Neumann boundary condition. Hence one can consider our results as an extension of the validity of the result from [6].

The authors thank anonymous referees for helpful comments.

References

1. P. R. Wallace, Mathematical Analysis of Physical Problems, Dover, New York, 1984.
2. G. I. Barenblatt, Dynamics of turbulent spots and intrusions in stably stratified fluid, Izvestiya Akademii Nauk SSSR, Fizika Atmosphery i Okeana, 14 (1978), 195–206.
3. C. I. Christov and G. M. Homsy, Nonlinear dynamics of two-dimensional convection in a vertically stratified slot with and without gravity modulation, J Fluid Mech, 430 (2001), 335–360.
4. H. A. Levine, The quenching of solutions of linear parabolic and hyperbolic equations with nonlinear boundary conditions, SIAM J Math Anal, 14 (1983), 1139–1153.
5. K. Deng and M. Xu, Quenching for a nonlinear diffusion equation with a singular boundary condition, Z Angew Math Phys 50 (1999), 574–584.
6. M. Fila and H. A. Levine, Quenching on the boundary, Nonlinear Anal TMA, 21 (1993), 759–802.
7. A. A. Samarskii, The Theory of Difference Schemes, Marcel Dekker, New York, 2001.